RSC Advances

PAPER

View Article Online
View Journal | View Issue

Cite this: *RSC Adv.*, 2024, **14**, 38898

Synthesis, anticancer and antibacterial evaluation of novel spiramycin-acylated derivatives†

Zhiwei Wang, ‡[ab] Junxiang Cheng,‡[b] Hui Wen,[b] Tao Hou,[ab] Fengbin Luo,[b] Yaodong Wang,[b] Xingjun Xu, [ab] Yanfang Liu, [ab] Yaopeng Zhao*[ab] and Xinmiao Liang *[ab]

Spiramycin and its derivatives are commonly used antimicrobials, and its derivative, carrimycin, has recently been found to have good anticancer potential. Here, we found that the 4″-OH of spiramycin can be selectively acylated, resulting in a series of novel spiramycin derivatives with a structure similar to carrimycin. Anticancer studies showed that most of the derivatives exhibited moderate to good anti-proliferative activity against four cancer cell lines, including HGC-27, HT-29, HCT-116 and HeLa, especially compound **14**, which has the strongest activity against HGC-27 cells with an IC_{50} value of 0.19 ± 0.02 μM. Pharmacological studies on HGC-27 cells revealed that compound **14** could arrest the cell cycle in the S phase, raise ROS levels, and induce cell apoptosis *via* activation of Erk/p38 MAPK signaling pathways. In addition, antibacterial studies showed that most of the spiramycin I derivatives modified at the 4″-OH group enhanced antibacterial activity on the four tested strains, including *S. aureus*, *S. aureus* MRSA, *S. epidermidis*, and *B. subtilis*. In particular, compound **16** was the most effective one and comparable to linezolid, a commonly used first-line antimicrobial. These results suggest that spiramycin I derivatives may provide an opportunity to design new anticancer or antibacterial agents, even dual-function agents.

Received 27th April 2024
Accepted 28th October 2024

DOI: 10.1039/d4ra03126a

rsc.li/rsc-advances

Introduction

Spiramycin is a 16-membered macrolide antibiotic, produced by *Streptomyces ambofaciens* in the form of a mixture of three main compounds: spiramycins I, II and III,[1,2] of which spiramycin I is dominant (~80%) (Scheme 1).[3] As a widely used drug, spiramycin has potent antibacterial activity against most of Gram-(+) cocci and rods, mycoplasmas, and *Toxoplasma gondii*,[4,5] and exhibit good gastrointestinal tolerance, high affinity for tissues, and few adverse effects.[6,7] Several chemical modifications of spiramycin have been developed to improve its antibacterial properties, such as etherification, esterification or sulphonylation of the mycaminosyl-mycarose moiety and lactone ring,[8–11] *N*-demethylation or *N*-substitution of the forosamine and/or mycaminose moieties,[12] amination or alkenylation of the aldehyde,[13,14] and incorporation of nitrogen into the lactone macrocyclic ring.[15] Therein, Sano *et al.* found that 3,3″,4″-triacyl and 4″-substituted derivatives with relatively small acyl, sulfonyl and alkyl groups showed superior or comparable antibacterial effects to spiramycin I.[8,9,16] It is well known that many macrolide antibiotics have anticancer or synergistic anticancer effects, in addition to being antibacterial. For example, clarithromycin can suppress hepatocellular carcinoma, and azithromycin can enhance the anticancer activity of TRAIL (tumor necrosis factor-related apoptosis-inducing ligand).[17–22] Unlike those macrolide antibiotics, which have dual anti-infection and anticancer functions, spiramycin has only a weak anticancer effect in several human cancer cell lines with IC_{50} > 30 μM.[23]

Recently, carrimycin and its active ingredient isovalerylspiramycin I have received attention for their relatively potent anticancer effects in addition to being antibacterial.[24–27] Carrimycin is a genetically engineered macrolide antibiotic that can be regarded as a bio-derivative of spiramycin, mainly consisting of 4″-isovalerylspiramycin I, II, III (Scheme 1). Liang *et al.* reported that carrimycin can regulate the PI3K/AKT/mTOR and MAPK pathways, thus causing apoptosis of OSCC (oral squamous cell carcinoma) cells *in vitro* and *in vivo*.[24] Jin *et al.* further confirmed the anticancer capacity of carrimycin and its monomer (isovalerylspiramycin I) by inhibiting the proliferation, migration, and invasion of hepatocellular carcinoma cells.[25] Liu *et al.* reported that isovalerylspiramycin I could suppress non-small cell lung carcinoma (NSCLC) growth through ROS-mediated inhibition of PI3K/AKT signaling pathway.[26] Cui *et al.* showed that isovalerylspiramycin I could link the cancer

[a]*Key Lab of Phytochemistry and Natural Medicines, Dalian Institute of Chemical Physics, CAS, Dalian 116023, China. E-mail: ypzhao@dicp.ac.cn; liangxm@dicp.ac.cn; Fax: +86 411 84379539; Tel: +86 411 84379519*

[b]*Ganjiang Chinese Medicine Innovation Center, Nanchang, 330000, China*

† Electronic supplementary information (ESI) available. See DOI: https://doi.org/10.1039/d4ra03126a

‡ Zhiwei Wang and Junxiang Cheng were contributed equally to this work.

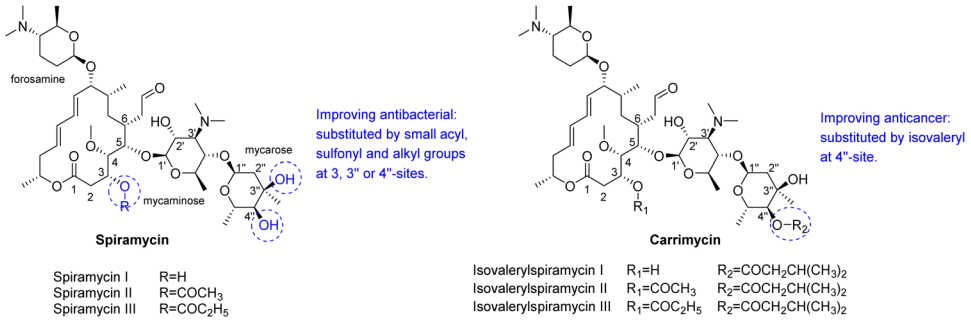

Scheme 1 Structures of main components of spiramycin and carrimycin, and some known structure–activity relationships.

cell vulnerability to oxidative stress and RNA biogenesis by targeting the nucleolar protein selenoprotein H.[27] Based on these results, further exploration of the anticancer potential of spiramycin derivatives is encouraged.

However, the anticancer potency of most known spiramycin derivatives to date remains moderate or weak, and their structural diversity is also very limited, which limits their drug development. Here, we are very interested in developing more spiramycin derivatives by means of chemical modification, and investigating their potential as both anticancer and antimicrobial agents.

Results and discussion

Chemistry

Spiramycin I has four hydroxyl groups, including 2′-, 3-, 3″- and 4″-OH (Scheme 1). Sano *et al.* reported that spiramycin I is esterified in a reactive order of 2′ > 4″ > 3 > 3″; therefore, the selective esterification of the 4″-OH group usually involves additional prior protection and subsequent deprotection of the 2′- and 3-OH groups.[9–11] To rapidly explore the modifiable scope of spiramycin I, we tried the direct esterification of spiramycin I. We first attempted the chemical synthesis of isovalerylspiramycin I using spiramycin I and isovaleryl chloride as starting materials. Results showed that by controlling the equivalent of isovaleryl chloride, a mono-isovalerylated spiramycin I (**1**) was obtained as the main product with a 30% yield. This was confirmed to be 4″-isovalerylspiramycin I by HPLC, HR-ESI-MS and NMR analysis (Fig. S2†). In another words, the main active component of carrimycin, 4″-isovalerylspiramycin I was chemically synthesized. This result is inconsistent with the order of hydroxyl activity in previous reports,[9] probably due to the use of a larger isovalery group, instead of the smaller substituents used by Sano *et al.* The steric hindrance of the 2′-OH was possibly larger than that of the 4″-OH group, leading to the isovaleryl group to preferentially bind to 4″-OH. Based on this finding, various acylated reagents with the number of carbon and heteroatoms ≥5 were selected to synthesize 4″-acylated sipramycin I derivatives **2–20** (Table 1).

Although only one mono-substituted product was obtained in most modification reactions, two mono-substituted products were obtained with comparable yields in the preparation of **9** (**9a**, 20% yield; **9b**, 20% yield) and **10** (**10a**, 25% yield; **10b**, 13% yield). 1D and 2D NMR studies of the two isomers **9a** and **9b** indicated that they were 3- and 4″-*p*-(*tert*-butyl)benzoyl spiramycin I, respectively (Fig. S3†). HPLC profile showed that **9a** had a shorter retention time than **9b** (Fig. S6†). Based on a similar HPLC analysis, **10a** and **10b** were attributed as 3- and 4″-*p*-butylbenzoyl spiramycin I, respectively. These results further contradicted the order of hydroxyl reactivity previously reported,[9] indicating that the steric hindrance of 3-OH is also smaller than that of 2′-OH. In addition to acyl chlorides and acids, several isocyanates can be used to react with spiramycin I to form 4″-carbamate derivatives **16–20**.

Pharmacology

Spiramycin I derivatives display anti-proliferation properties. Compounds **1–20** were first assessed for their anti-proliferation properties against human gastric cancer cell lines (HGC-27) (Table 2). The results showed that the compounds **1–5** with C5–C15 ester groups at the 4″-site of spiramycin I gave rise to moderate anti-proliferative activity ($3.96 \pm 0.17\ \mu M \leq IC_{50} \leq 8.08 \pm 0.30\ \mu M$). We suspected that appropriate hydrophobic properties may be an important factor in improving the activity of spiramycin ester derivatives. Surprisingly, compound **6**, which is only one nitrogen atom different from compound **1**, is almost inactive ($IC_{50} > 50\ \mu M$). We suspected that the amino group may be undesirable, but larger steric groups may weaken this adverse effect, which is why compound **7** has moderate activity with an IC_{50} of $5.78 \pm 0.15\ \mu M$. Some of the benzoate derivatives of spiramycin (compounds **8–10**) exhibited improved anti-proliferative activity, such as compound **9a** (IC_{50} $2.31 \pm 0.25\ \mu M$), **10a** (IC_{50} $1.66 \pm 0.29\ \mu M$) and **10b** (IC_{50} $0.92 \pm 0.06\ \mu M$). The comparison of two pairs of isomers of compounds **9** and **10** showed that whether the acylation was done at the 3-site or the 4″-site had little effect on the anti-proliferative activity of spiramycin I. Compounds **11–15** were then synthesized and tested. Encouragingly, their IC_{50} values were found to decrease to the submicromolar level ($0.19 \pm 0.02\ \mu M \leq IC_{50} \leq 1.20 \pm 0.17\ \mu M$), with compound **14**, being the most potent (IC_{50} $0.19 \pm 0.02\ \mu M$). Compounds **16** and **17** were structural analogues of compounds **2** and **4**, but their carbamate structure made them nearly inactive (both $IC_{50} > 50\ \mu M$). The *p*-methoxylphenylcarbamate derivative **18** was also inactive ($IC_{50} > 50$

Table 1 3- or 4″-Acylated derivatives of spiramycin I

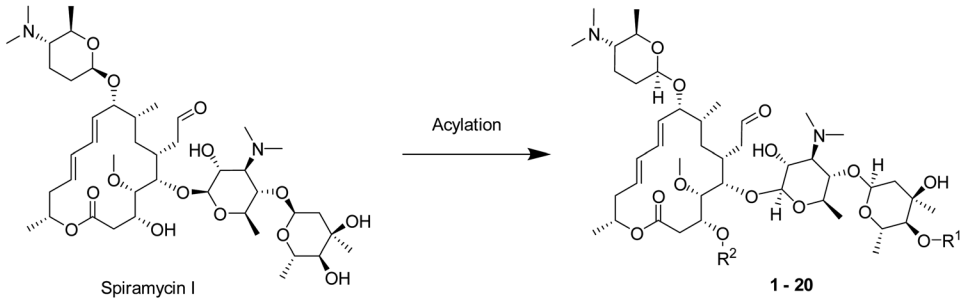

Acylation conditions: (1) acyl chloride, DMAP, Et_3N, DCM; (2) acid, DCC, 4-PPY, DMF; (3) isocyanates, Et_3N, DMF

Cmpd	R^1	R^2	Cmpd	R^1	R^2
1		H	**2**	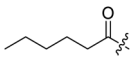	H
3	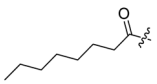	H	**4**		H
5	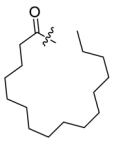	H	**6**	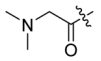	H
7	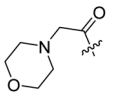	H	**8**	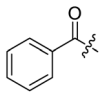	H
9a	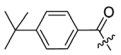	H	**9b**	H	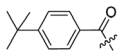
10a	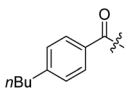	H	**10b**	H	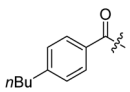
11	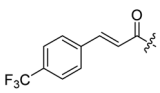	H	**12**	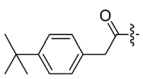	H
13	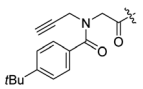	H	**14**	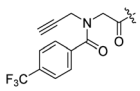	H
15	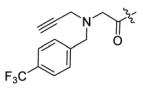	H	**16**	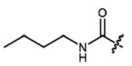	H
17	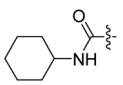	H	**18**	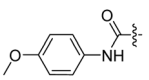	H
19	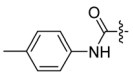	H	**20**	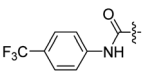	H

μM); however, the other two phenylcarbamate derivatives **19** and **20** exhibited moderate activity with IC_{50} values of 1.26 ± 0.19 and 1.76 ± 0.34 μM, respectively. In general, the aryl-acylated derivatives of spiramycin I appeared to have more potent anti-proliferative activity on HGC-27 cell lines than the alkyl-acylated derivatives.

Compounds **1–20** were further evaluated on three other human cancer cell lines (colorectal HT-29 and HCT-116, and

Table 2 IC_{50} values of compounds **1–20**, determined in various human cancer cell lines (HGC-27, HT-29, HeLa, HCT-116) and normal human gastric mucosa cell line (GES-1), with 5-FU as a positive control

	IC_{50} (μM)					
Cmpd	HGC-27	HT-29	HeLa	HCT-116	GES-1	SI (GES-1/HGC-27)
1	8.08 ± 0.30	13.15 ± 1.29	6.23 ± 0.36	12.66 ± 1.34	18.54 ± 2.56	2.29
2	5.23 ± 0.77	6.44 ± 0.36	23.67 ± 0.58	38.46 ± 6.36	38.82 ± 26.69	7.42
3	3.96 ± 0.17	5.42 ± 0.31	7.13 ± 0.24	10.62 ± 0.28	12.09 ± 0.60	3.05
4	4.27 ± 0.15	5.01 ± 0.28	8.50 ± 0.27	12.98 ± 0.30	14.51 ± 0.72	3.40
5	4.20 ± 0.08	3.94 ± 0.20	8.81 ± 0.17	14.56 ± 0.46	10.82 ± 0.35	2.58
6	>50	>50	>50	>50	>50	—
7	5.78 ± 0.15	4.19 ± 0.21	9.71 ± 0.31	8.0 ± 0.12	9.56 ± 0.323	1.65
8	5.31 ± 0.16	3.49 ± 0.16	7.18 ± 0.22	9.21 ± 0.14	13.08 ± 0.73	2.40
9a	2.31 ± 0.25	0.91 ± 0.02	1.30 ± 0.07	4.78 ± 0.52	3.34 ± 0.16	1.44
9b	7.97 ± 0.61	5.95 ± 0.61	26.37 ± 0.72	10.94 ± 0.23	31.25 ± 10.65	3.92
10a	1.66 ± 0.29	4.67 ± 0.40	4.22 ± 0.26	3.51 ± 0.49	2.75 ± 0.31	1.66
10b	0.92 ± 0.06	1.45 ± 0.12	1.00 ± 0.06	12.43 ± 0.68	4.68 ± 1.26	5.09
11	0.96 ± 0.20	2.32 ± 0.16	1.30 ± 0.08	2.36 ± 0.46	2.34 ± 0.36	2.44
12	0.49 ± 0.04	1.64 ± 0.13	2.05 ± 0.22	2.24 ± 0.45	2.29 ± 0.48	4.67
13	0.53 ± 0.15	1.84 ± 0.10	1.76 ± 0.70	10.98 ± 0.64	2.28 ± 0.47	4.30
14	0.19 ± 0.02	0.71 ± 0.06	1.24 ± 0.10	1.03 ± 0.05	1.96 ± 0.11	10.32
15	1.20 ± 0.17	2.15 ± 0.54	2.16 ± 0.44	4.39 ± 0.69	4.65 ± 0.18	3.88
16	>50	>50	>50	>50	>50	—
17	>50	>50	>50	>50	>50	—
18	>50	>50	>50	>50	>50	—
19	1.26 ± 0.19	3.27 ± 0.95	9.91 ± 0.66	22.01 ± 4.58	41.66 ± 13.93	33.06
20	1.76 ± 0.34	3.20 ± 0.24	2.29 ± 0.14	5.79 ± 0.38	6.64 ± 0.56	3.77
5-FU	4.75 ± 0.18	4.60 ± 0.55	3.43 ± 0.33	3.32 ± 0.30	4.03 ± 0.19	0.85

cervical HeLa) and one normal gastric epithelial cell line (GES-1). Results showed that these compounds also exhibited good to moderate anti-proliferative properties, but in general, most compounds were more sensitive to HGC-27 (Table 2). The selectivity index (SI) was calculated as the IC_{50} ratio of normal cells to cancer cells, SI = IC_{50} (GES-1)/IC_{50} (HGC-27). Results showed that compounds **14** and **19** had the highest selectivity against cancer cells, which suppressed the growth of HGC-27 cell lines with SI = 10.32 and 33.06, respectively. Considering the highest activity and selectivity, compound **14** was selected for further pharmacological studies on HGC-27.

Compound 14 promotes apoptosis of HGC-27 cells. Cell apoptosis is one of the major causes of cell proliferation inhibition. We next examined whether compound **14** can cause apoptosis of HGC-27 cells. Flow cytometry analysis showed that the apoptosis rate of HGC-27 cells increased from 8.87% to 70.90% with increasing concentrations of compound **14** (Fig. 1A and B). Western blot analysis showed that the levels of two apoptosis-related proteins, cleaved PARP and cleaved caspase-3, were significantly elevated with the increasing concentration of compound **14** (Fig. 1C and D). To summarize, these results suggested that compound **14** can induce cell apoptosis of HGC-27 cells.

Compound 14 arrests HGC-27 at cell cycle S. Aberrant cell cycle always occurred in tumor cells. We performed cell cycle analysis after HGC-27 cells treated with compound **14** (Fig. 2A and B). Results showed that after treatment with increasing concentrations of compound **14** for 48 h, the proportion of S phase significantly increased from 28.23% to 37.77% while the proportions of both G0/G1 and G2/M phases decreased. Western blot showed that the level of the tumor suppressor p53 increased after the treatment of compound **14**, while the levels of two S phase-related key proteins CDK2 and Cyclin A considerably decreased in a concentration-dependent manner (Fig. 2C and D). These data suggested that compound **14** preferably arrests HGC-27 cells at the S phase, different from those of carrimycin or compound **1** reported in literature, which arrest OSCC or NSCLC cells at G0/G1 or G2/M phase, respectively.[24,26]

Compound 14 raises ROS levels in HGC-27 cells. Given that compound **1** could induce NSCLC apoptosis through ROS accumulation,[17] we further evaluated the effects of compound **14** on ROS in HGC-27 cells. DCFH-DA, a fluorescence probe for ROS detection, was employed to evaluate the level of intracellular ROS. HGC-27 cells were incubated with compound **14** for 24 h, followed by treatment with DCFH-DA for 30 min to mark the induced intracellular ROS. Results showed that compound **14** considerably raised the ROS levels in a concentration-dependent manner ranging from 0.45 to 1.80 μM (Fig. 3A). Furthermore, the addition of the ROS scavenger NAC could effectively decrease ROS accumulation, causing the shift in the IC_{50} value of compound **14** from 0.219 μM to 1.805 μM (Fig. 3B). We also examined and found nearly no change of the mitochondrial membrane potential and related marker proteins Bax and Bcl-2 of HGC-27 (Fig. S6†). To summarize,

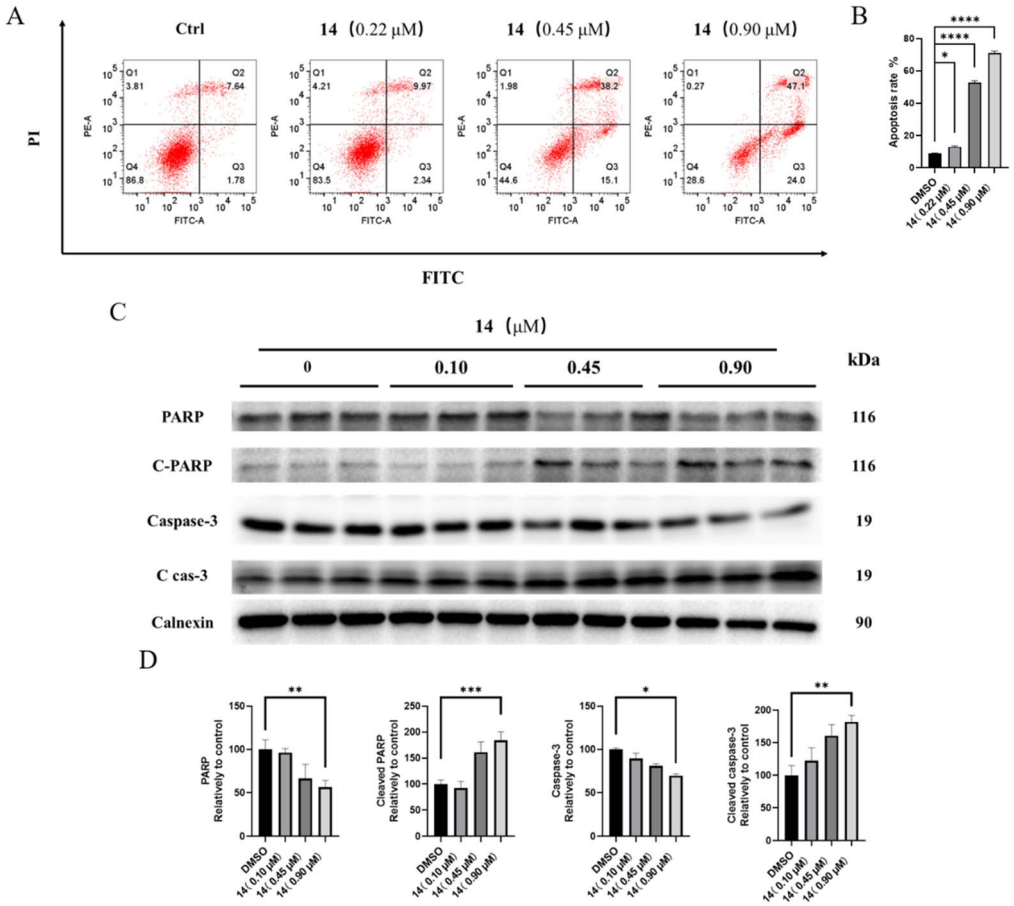

Fig. 1 Compound **14** induced apoptosis of HGC-27 cells. (A) Flow cytometry and (B) bar graph analysis of cell apoptosis in HGC-27 after treatment with **14** (0, 0.22 0.45, 0.9 μM) for 72 h. (C) Western blot images and (D) bar graph analysis of PARP, cleaved PARP, caspase-3 and cleaved caspase-3 protein expressions in HGC-27 after treatment with **14** (0, 0.10, 0.45, 0.90 μM) for 24 h, $*p < 0.05$; $**p < 0.01$; $***p < 0.001$.

these results suggest that **14** can raise the ROS levels in HGC-27 cells.

Compound 14 induces Erk/p38 signaling pathway in HGC-27 cells. We further investigated the anti-proliferation signaling pathways of compound **14** on HGC-27 cells. The mitogen-activated protein kinase (MAPK) pathway is related to many physiological effects, including apoptosis and cell proliferation. We examined the activation of MAPKs, including Erk1/2 and p38, by compound **14** in HGC-27 cells using western blot analysis. Results showed that p-Erk1/2 and p-p38 levels significantly increased in compound **14** treated cells, while Erk1/2 levels and p38 levels remained the same (Fig. 4A and B). These results indicated that compound **14** induce HGC-27 apoptosis *via* Erk/p38 signaling pathway.

Spiramycin I derivatives improve antibacterial activity. Some spiramycin I derivatives were selected for antibacterial evaluation against four common strains (Table 3 and Fig. S7†). The results showed that most compounds, including compounds **6**, **16** and **17** with no anti-proliferative activity, gave rise to considerable antibacterial activity on the four strains (MIC 2–32 μM). Notably, compounds **9a** and **11** had no antibacterial activity on the *S. aureus* strain (MIC > 128 μM). As the main antibacterial active component of carrimycin, isovaleryl-modified compound **1**, showed more potent antibacterial effects than spiramycin I against all four strains (MIC 4–16 μM). Compared with compound **1**, the *n*-hexanoyl-modified compound **2** further enhanced its activity (MIC 2–8 μM), but further extension of the carbon chain (*e.g.* **5** with MIC 4–32 μM) or substitution of aromatic groups (*e.g.* **9–15** with MIC 4–32 μM) decreased the activities. As an analog of compound **2** doped with the N atom, the *n*-butylcarbamate-modified compound **16** showed stronger antibacterial activities against *S. epidermidis* and *B. subtilis*, and the two MIC reached 1 μM, respectively. It is impressive that compound **16** achieved antimicrobial levels on all four strains comparable to that of linezolid, a potent antimicrobial drug widely used clinically against Gram-positive bacteria. Among these spiramycin I derivatives, compound **14**, which exhibited the strongest anti-proliferative activity, showed only moderate antibacterial activity (MIC 4–16 μM), while compound **16**, with the strongest antibacterial activity, had no significant anti-proliferative activity. These results suggested that the antimicrobial and anti-proliferative properties have distinct structural preferences for these spiramycin I derivatives.

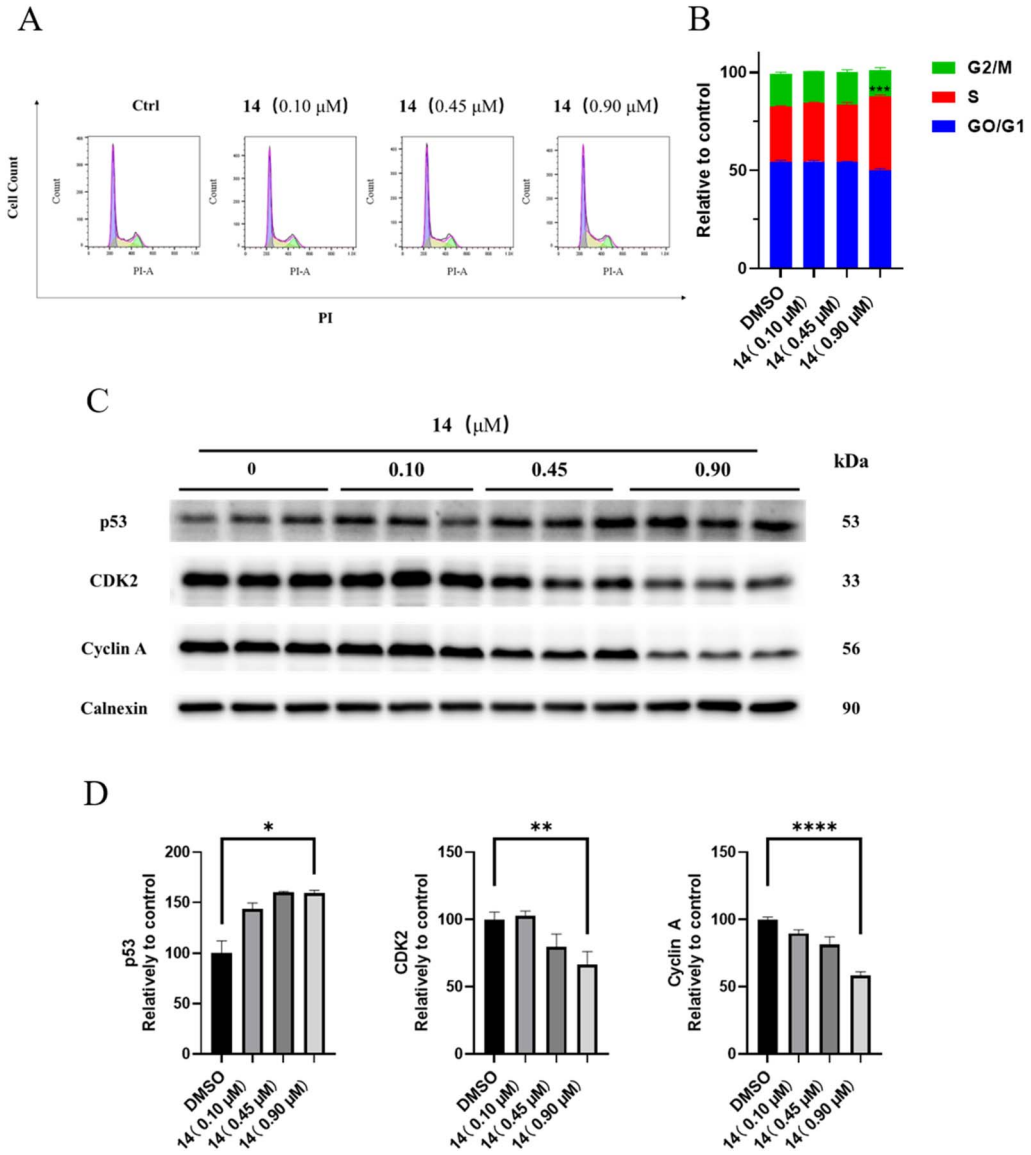

Fig. 2 The effect of compound **14** on HGC-27 cell cycle. (A) Flow cytometry and (B) bar graph analysis of cell cycle distribution in HGC-27 after treatment with compound **14** (0, 0.10, 0.45, 0.90 μM) for 48 h. (C) Western blot images and (D) bar graph analysis of p53, CDK2 and Cyclin A protein expressions in HGC-27 after treatment with compound **14** (0, 0.10, 0.45, 0.90 μM) for 24 h. *$p < 0.05$; **$p < 0.01$; ****$p < 0.0001$.

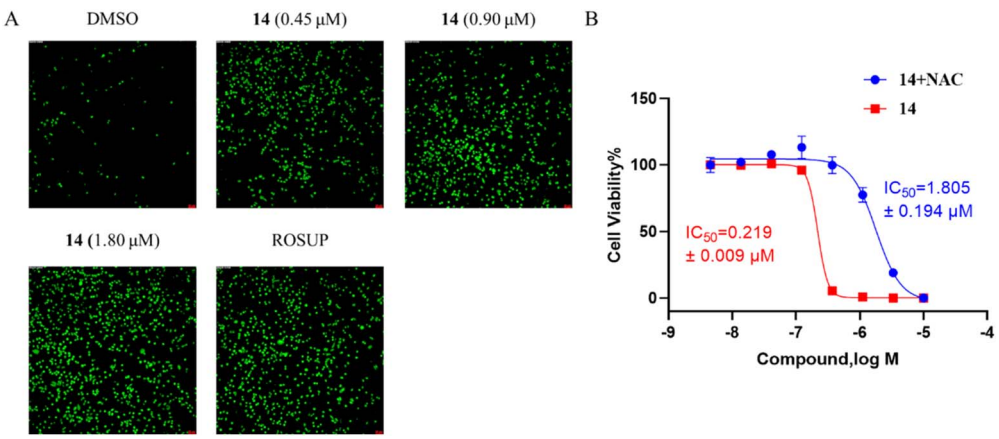

Fig. 3 The effect of compound **14** on HGC-27 cell ROS generation. (A) Detection of ROS generation by DCFH-DA in HGC-27 cells after incubation with compound **14** (0, 0.45, 0.90, 1.80 μM) for 48 h, (B) ROS scavenger NAC increase the IC_{50} value of compound **14**.

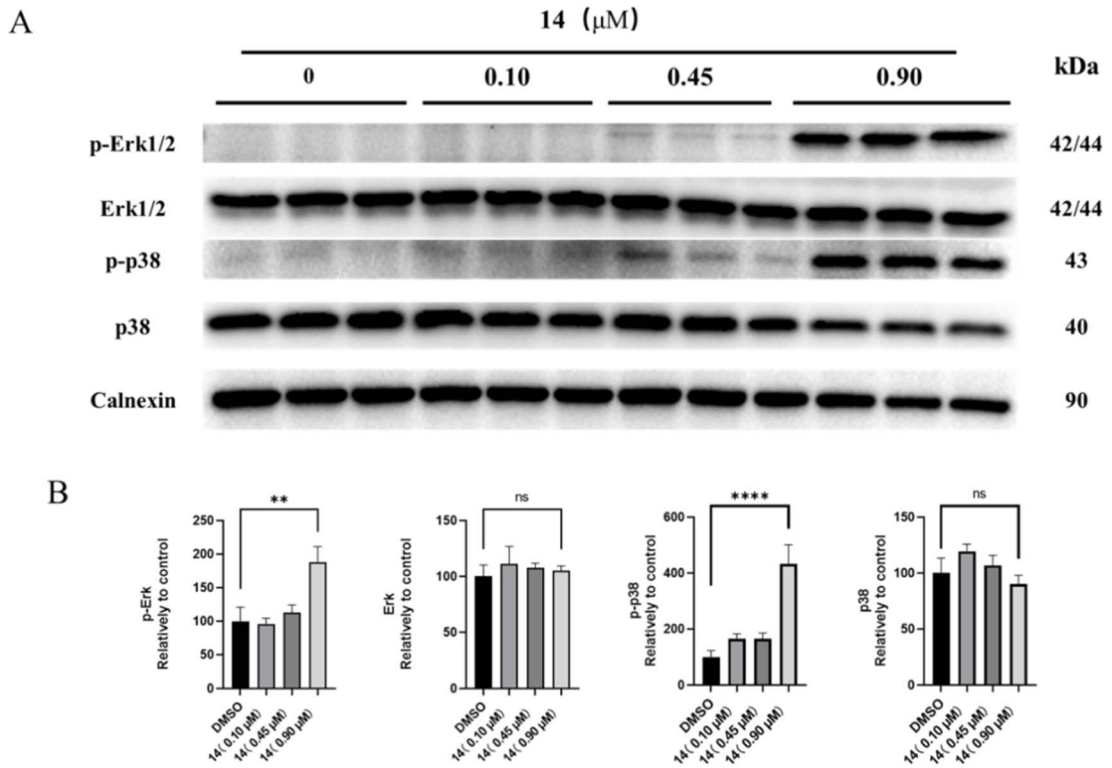

Fig. 4 The effect of compound **14** on Erk/p38 MAPK signaling pathways. (A) Western blot images of Erk1/2, p-Erk1/2, p38 and p-p38 protein expressions in HGC-27 after treatment with (A) compound **14** (0, 0.10, 0.45, 0.90 μM) for 24 h. (B) Corresponding bar graph analysis of the signaling pathways. $^{**}p < 0.01$; $^{****}p < 0.0001$.

Table 3 MIC values of selected spiramycin I derivatives, expressed in μg mL^{-1}, and in μM, evaluated in the 0.5–128 μM range of concentrations

	S. aureus ATCC25923	*S. aureus* MRSA ATCC515992	*S. epidermidis* ATCC12228	*B. subtilis* ATCC6633
Spiramycin I	53.96 [64]	53.96 [64]	13.49 [16]	13.49 [16]
1	7.40 [8]	14.80 [16]	3.70 [4]	3.70 [4]
2	3.77 [4]	7.54 [8]	3.77 [4]	1.89 [2]
3	7.75 [8]	15.51 [16]	7.75 [8]	1.94 [2]
4	7.63 [8]	15.25 [16]	3.81 [4]	3.81 [4]
5	14.85 [16]	29.70 [32]	7.43 [8]	3.71 [4]
6	7.76 [8]	15.52 [16]	7.76 [8]	1.94 [2]
9a	>128.42 [>128]	16.05 [16]	4.01 [4]	4.01[4]
10a	8.02 [8]	32.08 [32]	4.01 [4]	4.01 [4]
10b	16.04 [16]	16.04 [16]	8.02 [8]	2.00 [2]
11	>133.12 [>128]	33.30 [32]	4.16 [4]	8.32 [8]
12	8.13 [8]	16.27 [16]	4.07 [4]	4.07 [4]
13	17.56 [16]	35.12 [32]	8.78 [8]	4.39 [4]
14	17.75 [16]	17.75 [16]	8.88 [8]	4.44 [4]
16	3.87 [4]	7.75 [8]	0.97 [1]	0.97 [1]
17	15.61 [16]	62.44 [64]	7.80 [8]	15.61 [16]
20	8.24 [8]	32.97 [32]	8.24 [8]	2.06 [2]
Linezolid	1.35 [4]	2.67 [8]	0.34 [1]	0.17 [0.5]

Conclusion

In conclusion, we found that the 4″-OH of spiramycin I can be preferably acylated under controlled conditions, leading to the preparation of 21 novel spiramycin I derivatives, which greatly expand its chemical space. More importantly, the 4″-OH acylation greatly improves its anti-proliferative activity across four different cancer cell lines. The structure–activity relationship study indicated that the aryl-acylated derivatives of spiramycin I appear to have more potent anti-proliferative activity against the HGC-27 cell line compared to the alkyl-acylated derivatives. The most potent anti-proliferative compound **14**

was found to arrest the HGC-27 cell cycle in the S phase, increase ROS levels, inhibit the phosphorylation of Erk and p38, thus lead to the apoptosis of HGC-27 cells. In addition to its anti-proliferative activity, most of these derivatives gave rise to enhanced antibacterial activity against four common strains compared to spiramycin I. Therein, compound **16** showed very potent antimicrobial activity comparable to that of linezolid. Considering that patients with malignant tumors are more likely to develop infection during surgery, drugs that have the dual functions of anticancer and antibacterial appear to be very advantageous in cancer treatment.

Experimental

Chemistry

General. ^{1}H and ^{13}C NMR spectra were obtained at 400/600 and 101/151 MHz, respectively, using a Brucker AVANCE400/600 spectrometer. Chemical shifts were reported in ppm relative to TMS as the internal standard. LC-MS spectra were measured on a combined system consisting of a Waters Alliance e2695, Waters 2998 PDA and Waters QDA. High-resolution mass spectrometry (HRMS) was performed using an Agilent 1290 Infinity LC system (Agilent, USA) coupled to an Agilent 6540 series QTOF-MS (Agilent, USA) equipped with an ESI† source, a diode-array detector (DAD), an automatic sample injector, a degasser and a column thermostat. Flash chromatography and thin-layer chromatography were done using silica gel 60 (300–400 mesh) from Qingdao Haiyang Chemical Co., Ltd. Standard solvents from Sinopharm Chemical Reagent Co., Ltd were used as received. Anhydrous solvents were treated using standard methods, and all other commercially available reagents were used without further purification. Yields were not optimized.

Method A: general synthesis procedure by using acyl chloride reagents. Spiramycin I (0.5 mmol, 1.0 equiv.) and the appropriate acyl chloride reagent (1.0 mmol, 2.0 equiv.) were dissolved in 10 ml of DCM. To this solution, *N*,*N*-dimethylaminopyridine (DMAP, 1.0 mmol, 2.0 equiv.) and triethylamine (TEA, 1.0 mmol, 2.0 equiv.) were added, and the mixture was stirred at 30 °C for 24 h. Once the acyl chloride reagent was completely consumed, the reaction mixture was concentrated under reduced pressure. The oil residue was purified by flash silica chromatography using a 5% ACN/CH_2Cl_2 eluent. The resulting crude product was further purified by a C18 pre-HPLC to give the target products.

Method B: general synthesis procedure using acid reagents. Spiramycin I (0.5 mmol, 1.0 equiv.) and the appropriate carboxylic acid (1.0 mmol, 2.0 equiv.) were dissolved in 10 ml DMF. To this solution, dicyclohexylcarbodiimide (DDC, 0.5 mmol, 1.0 equiv.) and 4-pyrrolidinopyridine (4-PPY, 0.25 mmol, 0.5 equiv.) were added, and the resulting mixture was stirred at 30 °C for 24 h. When the reaction was finished, the mixture was concentrated under reduced pressure. The oil residue was purified by flash silica chromatography using a 5% ACN/CH_2Cl_2 eluent. The resulting crude product was further purified by C18 pre-HPLC to give the target products.

Method C: general synthesis procedure by using isocyanate reagents. Spiramycin I (0.5 mmol, 1.0 equiv.) and the appropriate isocyanate (1.0 mmol, 2.0 equiv.) were dissolved in 10 ml of DMF. To this solution, triethylamine (TEA, 1.0 mmol, 2.0 equiv.) was added, the resulting mixture was stirred at 30 °C for 24 h. When the reaction was finished, the mixture was concentrated under reduced pressure. The oil residue was purified by flash silica chromatography using a 5% ACN/CH_2Cl_2, eluent. The resulting crude product was further purified by C18 pre-HPLC to give the target products.

Biology

Reagents, cell lines and bacteria strains. Cancer cell lines HGC-27, HT-29, HeLa, HCT-116 and the normal cell line GES-1 were purchased from the National Collection of Authenticated Cell Cultures (Shanghai, China). Fetal bovine serum (FBS), penicillin–streptomycin, and trypsin were purchased from Thermo Fisher Scientific Inc (Waltham, USA). Bacteria strains *S. aureus* ATCC25923, *S. aureus* MRSA ATCC515992, *S. epidermidis* ATCC12228 and *B. subtilis* ATCC6633 were purchased from BeNa Culture Collection (Beijing, China). MH broth and NB broth were also purchased from BeNa Culture Collection (Beijing, China). WST-8 and 5-FU were purchased from Yuanye Biotechnology (Shanghai, China). Protease inhibitors, phosphatase inhibitors, western blocking buffer, enhanced BCA protein assay kit, SDS-PAGE gel kit, BeyoECL Plus kit, Annexin V-FITC cell apoptosis detection kit and PI cell cycle detection kit were purchased from Beyotime Biotechnology (Shanghai, China). TBST buffer, glycine, Tris and SDS were purchased from Solarbio (Beijing, China). Antibodies against Erk1/2, p-Erk1/2, p38, p-p38, caspase-3, cleaved caspase-3, PARP, cleaved PARP, GAPDH, tubulin, anti-mouse IgG-HRP-linked antibody, and anti-rabbit IgG-HRP-linked antibody were purchased from Cell Signaling Technology (Boston, USA). Antibodies against p53, CDK2, Cyclin A and Calnexin were purchased from Proteintech (Wuhan, China).

Cell culture and anti-proliferation assay. HGC-27 and GES-1 were cultured in the RPMI 1640 medium. HT-29 and HCT116 were cultured in the McCoy's 5A medium. HeLa cells were cultured in the DMEM medium. All cell culture media contained 10% FBS and 1% penicillin–streptomycin. All cell lines were cultured in 5% CO_2 incubator at 37 °C. When the cell confluency reached more than 80%, cells were digested and plated on 96 well plates (4000 cells per well), then incubated overnight for adherence. Different concentrations of 5-FU (0–50 μM, 2-fold dilutions) and derivatives (0–500 μM, 3-fold dilutions) were added to each well to measure the anti-proliferation ability. After 72 h treatment, old media was exchanged with the fresh media containing cell counting kit (CCK8, consist 0.5 mM wst-8 and 10 μM pms). After 0.5–2 h incubation, absorbance at wavelength 450 nm was recorded by the microplate reader. The cell viability and anti-proliferative activity were calculated.

Cell cycle distribution assay. The effects of compound **14** on cell cycle distribution were determined by flow cytometry. HGC-27 was seeded in 6-well plates (2×10^5 cells per well) and incubated overnight for adherence. Then, cells were treated with compound **14** (0, 0.10, 0.45, 0.90 μM) for 48 h. After

treatment, cells were harvested, fixed in 70% ethanol for 1 h at 4 °C, and stained with a solution containing PI and RNase for 0.5 h. The stained cells were then examined on a FACS Calibur flow cytometer using CellQuest Pro software (BD Biosciences, California, USA). The percentage of cells in different phases of the cell cycle was determined using FlowJo software (BD Biosciences).

Cell apoptosis assay. The effects of compound **14** on cell apoptosis were determined by flow cytometry. HGC-27 cells were seeded in 6-well plates (2×10^5 cells per well) and incubated overnight for adherence. Then, cells were treated with compound **14** (0, 0.22, 0.45, 0.9 μM) for 48 h. After treatment, cells were harvested and stained with a solution containing Annexin V-FITC and PI for 0.5 h. The stained cells were then examined using a FACS Calibur flow cytometer with CellQuest Pro software (BD Biosciences). The percentage of apoptosis population was determined using FlowJo software (BD Biosciences).

Western blot assay. HGC-27 were seeded in 6 well plates (1×10^6 cells per well) and incubated overnight for adherence. Then, cells were treated with compound **14** (0, 0.10, 0.45, 0.9 μM) for 24 h. Cells were harvested and lysed with RIPA lysis buffer containing protease and phosphatase inhibitors. Lysates were centrifuged for 10 min at 15 000 rpm, and the supernatants were collected. Total protein concentration were measured using the enhanced BCA protein assay kit. Equal amounts of protein (20–50 μg) were loaded onto an SDS-PAGE gel (8%, 10%, 12%, 15%). After electrophoresis, the gels were transferred to a polyvinylidene difluoride (PVDF) membrane, which was then blocked by western blocking buffer for 1 h. Then PVDF membranes were interacted with primary antibodies overnight at 4 °C, and washed three times for 10 min in 1× TBST solution. After that, PVDF membranes were mixed with peroxidase-labeled secondary antibodies for 1 h at room temperature, then washed three times for 10 min in 1× TBST solution. Protein bands were acquired using BeyoECL Plus kit by ChemiDocTM XRS+ (Bio-Rad, California, USA). Band intensities were quantified using the Image J (National Institute of Health, Maryland, USA).

ROS detection assay and NAC inhibition assay. HGC-27 were seeded in 96 well plates (1×10^4 cells per well) and incubated overnight for adherence. Then, cells were treated with compound **14** (0, 0.45, 0.90, 1.80 μM) for 24 h. As control, cells were treated with ROSUP (50 μg mL^{-1}) for 0.5 h. After treatment, DCFH-DA was added for ROS detection, the green fluorescence was observed using IFM (Leica, Wetzlar, German). HGC-27 were seeded in 96-well plates (4×10^3 cells per well) and incubated overnight for adherence. Then, cells were treated with different compounds (group compound **14** cell were only treated with compound **14**, group Cotreat cells were treated with compound **14** and 3 mM NAC). Cell viability was measured using the CCK8 assay and the IC_{50} was calculated after 72 h.

Bacterial culture and MIC assay. S. aureus ATCC25923, *S. aureus* MRSA ATCC515992, and *B. subtilis* ATCC6633 were cultured in MH broth, while *S. epidermidis* ATCC12228 was cultured in NB broth. All bacterial strains were cultured at 37 °C under aerobic conditions. Concentrated solutions of the tested compounds (positive control linezolid) were dissolved in DMSO and diluted in MH/NB broth to obtain the required concentrations (0.5–128 μM). Four bacterial strains were diluted (final concentration $OD_{600} = 0.05$) and plated in 96-well plate. Different concentrations of the tested compounds were added to each well. The minimal inhibitory concentration (MIC) was determined after 18 h of incubation at 37 °C.

Data availability

All relevant data are within the manuscript and its additional files.

Conflicts of interest

There are no conflicts to declare.

Acknowledgements

The authors would like to extend their sincere appreciation to the Jiangxi Provincial Natural Science Foundation (20224BAB216003).

References

1 A. Thibessard, D. Haas, C. Gerbaud, B. Aigle, S. Lautru, J. L. Pernodet and P. Leblond, *J. Biotechnol.*, 2015, **214**, 117–118.
2 T. Mazzei, E. Mini, A. Novelli and P. Periti, *J. Antimicrob. Chemother.*, 1993, **31**(Suppl C), 1–9.
3 L. Liu, E. Roets and J. Hoogmartens, *J. Chromatogr. A*, 1997, **764**, 43–53.
4 K. Ramu, S. Shringarpure and J. S. Williamson, *Pharm. Res.*, 1995, **12**, 621–629.
5 T. Miura, K. Kanemoto, S. Natsume, K. Atsumi, H. Fushimi, T. Yoshida and K. Ajito, *Bioorg. Med. Chem.*, 2008, **16**, 10129–10156.
6 E. Rubinstein and N. Keller, *J. Antimicrob. Chemother.*, 1998, **42**, 572–576.
7 M. A. Pilot and X. Y. Qin, *J. Antimicrob. Chemother.*, 1988, **22**(Suppl B), 201–206.
8 H. Sano, T. Sunazuka, H. Tanaka, K. Yamashita, R. Okachi and S. Omura, *J. Antibiot.*, 1984, **37**, 750–759.
9 H. Sano, T. Sunazuka, H. Tanaka, K. Yamashita, R. Okachi and S. Omura, *J. Antibiot.*, 1984, **37**, 760–772.
10 M. Sano, T. Sunazuka, H. Tanaka, K. Yamashita, R. Okachi and S. Omura, *J. Antibiot.*, 1985, **38**, 1350–1358.
11 T. Hirose, T. Sunazuka, Y. Noguchi, Y. Yamaguchi, H. Hanaki, K. B. Sharpless and S. Omura, *Heterocycles*, 2006, **69**, 55–61.
12 H. Sano, H. Tanaka, K. Yamashita, R. Okachi and S. Omura, *J. Antibiot.*, 1985, **38**, 186–196.
13 K. I. Rivera-Márquez, C. Godoy-Alcántar, M. Á. Claudio-Catalán and F. Medrano, *J. Inclusion Phenom. Macrocyclic Chem.*, 2016, **86**, 211–219.
14 S. K. Murphy, J. W. Park, F. A. Cruz and V. M. Dong, *Science*, 2015, **347**, 56–60.

15 G. Castro-Falcón, N. Millán-Aguiñaga, C. Roullier, P. R. Jensen and C. C. Hughes, *ACS Chem. Biol.*, 2018, **13**, 3097–3106.
16 H. Takahira, *Jpn. J. Antibiot.*, 1970, **23**, 424–428.
17 U. Galm, M. H. Hager, S. G. Van Lanen, J. Ju, J. S. Thorson and B. Shen, *Chem. Rev.*, 2005, **105**, 739–758.
18 A. Hussain, M. S. Dar, N. Bano, M. M. Hossain, R. Basit, A. Q. Bhat, M. A. Aga, S. Ali, Q. P. Hassan and M. J. Dar, *Cancer Chemother. Pharmacol.*, 2019, **84**, 551–559.
19 X. Qiao, X. Wang, Y. Shang, Y. Li and S. Z. Chen, *Cancer Commun.*, 2018, **38**, 43.
20 X. Zhou, Y. Zhang, Y. Li, X. Hao, X. Liu and Y. Wang, *Cancers*, 2012, **4**, 1318–1332.
21 N. I. Abdel-Hamid, M. F. El-Azab and Y. M. Moustafa, *Naunyn-Schmiedeberg's Arch. Pharmacol.*, 2017, **390**, 379–395.
22 R. Lamb, B. Ozsvari, C. L. Lisanti, H. B. Tanowitz, A. Howell, U. E. Martinez-Outschoorn, F. Sotgia and M. P. Lisanti, *Oncotarget*, 2015, **6**, 4569–4584.
23 K. Klich, K. Pyta, M. M. Kubicka, P. Ruszkowski, L. Celewicz, M. Gajecka and P. Przybylski, *J. Med. Chem.*, 2016, **59**, 7963–7973.
24 S. Y. Liang, T. C. Zhao, Z. H. Zhou, W. T. Ju, Y. Liu, Y. R. Tan, D. W. Zhu, Z. Y. Zhang and L. P. Zhong, *Transl. Oncol.*, 2021, **14**, 101074.
25 Y. Jin, H. X. Zuo, M. Y. Li, Z. H. Zhang, Y. Xing, J. Y. Wang, J. Ma, G. Li, H. Piao, P. Gu and X. Jin, *Front. Pharmacol*, 2021, **12**, 774231.
26 Z. Liu, M. Huang, Y. Hong, S. Wang, Y. Xu, C. Zhong, J. Zhang, Z. Zhuang, S. Shan and T. Ren, *Int. J. Biol. Sci.*, 2022, **18**, 3714–3730.
27 J. Cui, J. Zhou, W. He, J. Ye, T. Westlake, R. Medina, H. Wang, B. L. Thakur, J. Liu, M. Xia, Z. He, F. E. Indig, A. Li, Y. Li, R. J. Weil, M. I. Aladjem, L. Zhong, M. R. Gilbert and Z. Zhuang, *J. Exp. Clin. Cancer Res.*, 2022, **41**, 126.